

$X(3872)$ and the search for its bottomonium counterpart at the LHC

Konstantin Toms
on behalf of the ATLAS, CMS, and LHCb Collaborations

University of New Mexico

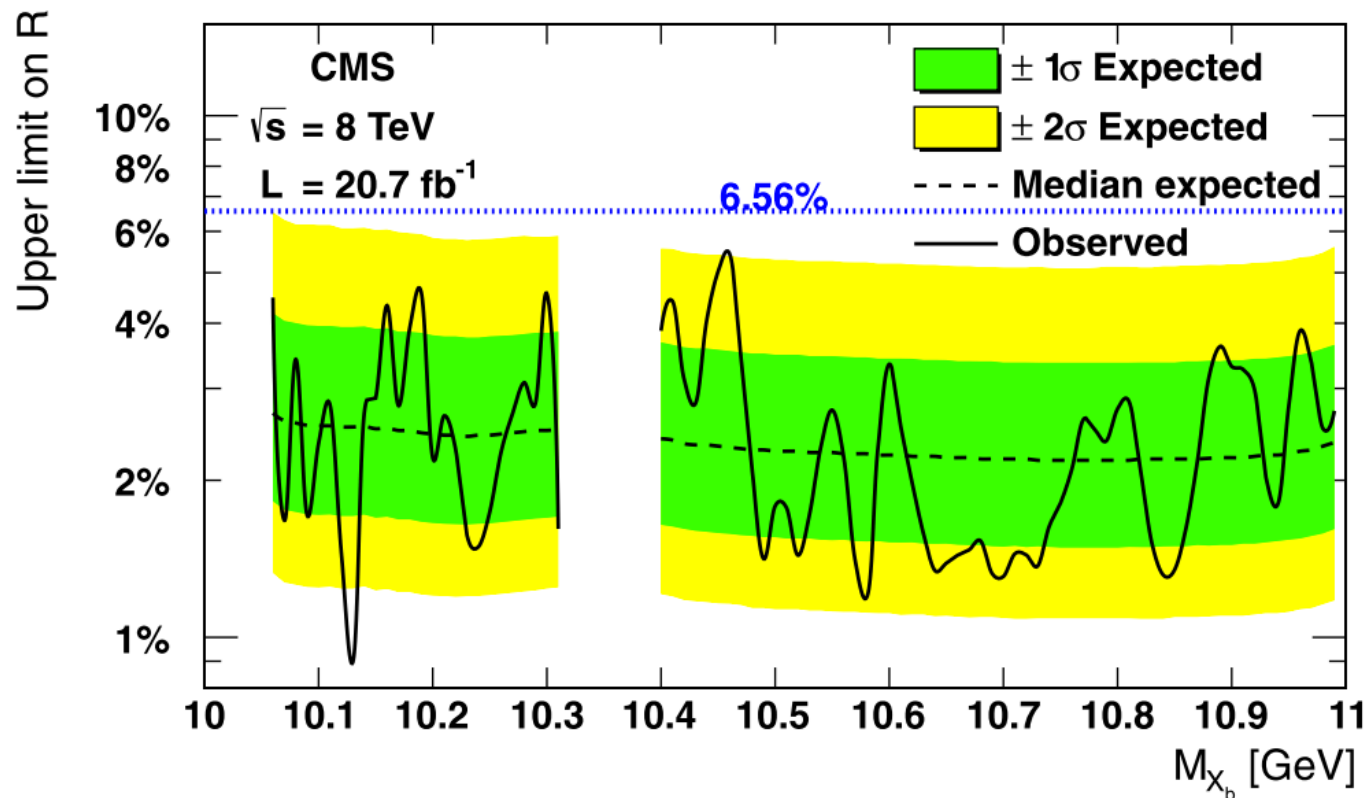
Outline

- Brief $X(3872)$ history and theoretical status overview.
- Search for $X(3872)$ bottomonium counterpart, X_b at CMS.
- Search for the X_b by ATLAS and study of the $\psi(2S)$ and $X(3872)$ production.
- Determination of $X(3872)$ quantum numbers at LHCb.

X(3872) history and theoretical status overview

- X(3872) was first discovered by Belle in 2003 in $B^{+,0} \rightarrow X(3872)K^{+,0}$, $X(3872) \rightarrow \pi^+\pi^-J/\psi$, $J/\psi \rightarrow \ell^+\ell^-$ and soon confirmed by many experiments.
- The X(3872) state is narrow, has a mass very close to the $D^0\bar{D}^{*0}$ threshold and decays to ρ^0J/ψ and $\omega J/\psi$ final states with comparable branching fractions, thus violating isospin symmetry \rightarrow not a simple $c\bar{c}$ state.
- The structure of the state remains unclear, there are lots of theoretical developments in the area: tetraquark, molecular, and mixed models.
- Searches for the bottomonium counterpart are now very active.
- Previous and recent X(3872) analyses by CMS and LHCb:
 - [Eur. Phys. J. C \(2012\) 72: 1972](#), LHCb, observation of X(3872) production.
 - [JHEP 04 \(2013\) 154](#), CMS, measurement of the X(3872) production cross section.
 - [Nucl. Phys. B 886 \(2014\) 665-680](#), LHCb, evidence for the decay $X(3872) \rightarrow \psi(2S)\gamma$.
 - [arXiv:1607.06446 \(2016\)](#), LHCb, observation of $\eta_c(2S) \rightarrow p\bar{p}$ and search for $X(3872) \rightarrow p\bar{p}$ decays.

Search for the X_b at CMS

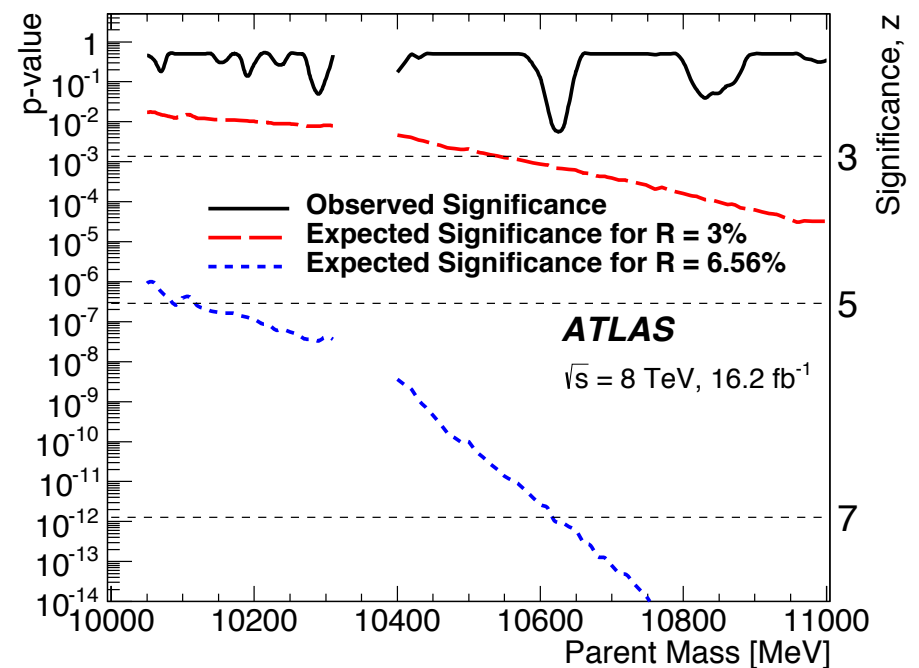
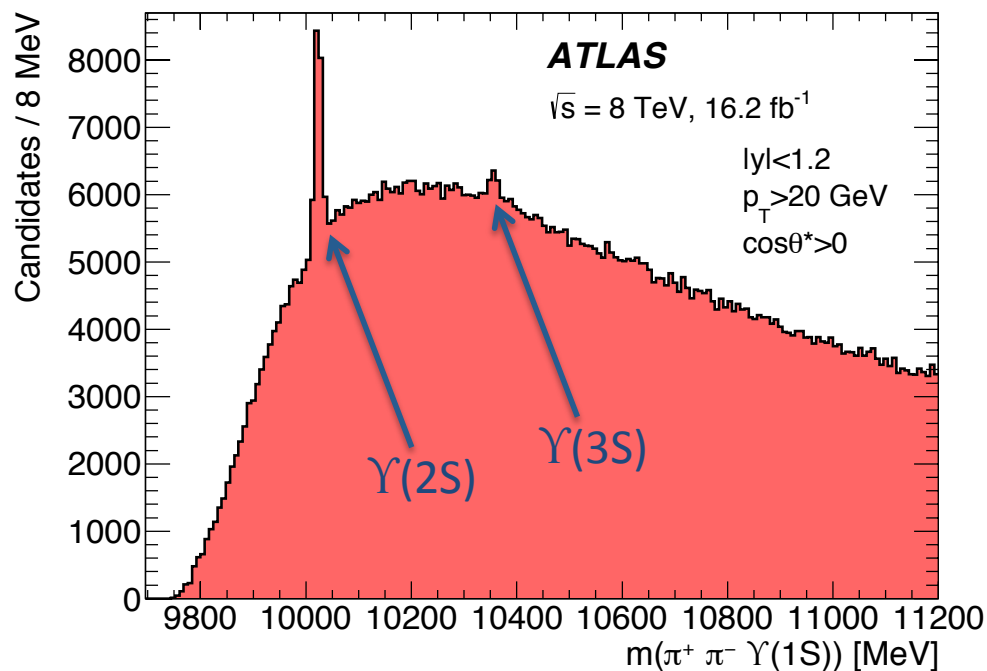


- [Phys. Lett. B 727 \(2013\), pp. 57–76](#)
- 20.7 fb⁻¹ of 8 TeV CMS data.
- No evidence for X_b is observed.
- Upper limits are set at the 95% confidence level on the ratio of the inclusive production cross sections times the branching fractions to $\Upsilon(1S)\pi^+\pi^-$ of the X_b and the $\Upsilon(2S)$. The upper limits on the ratio are in the range 0.9–5.4% for X_b masses between 10 and 11 GeV.

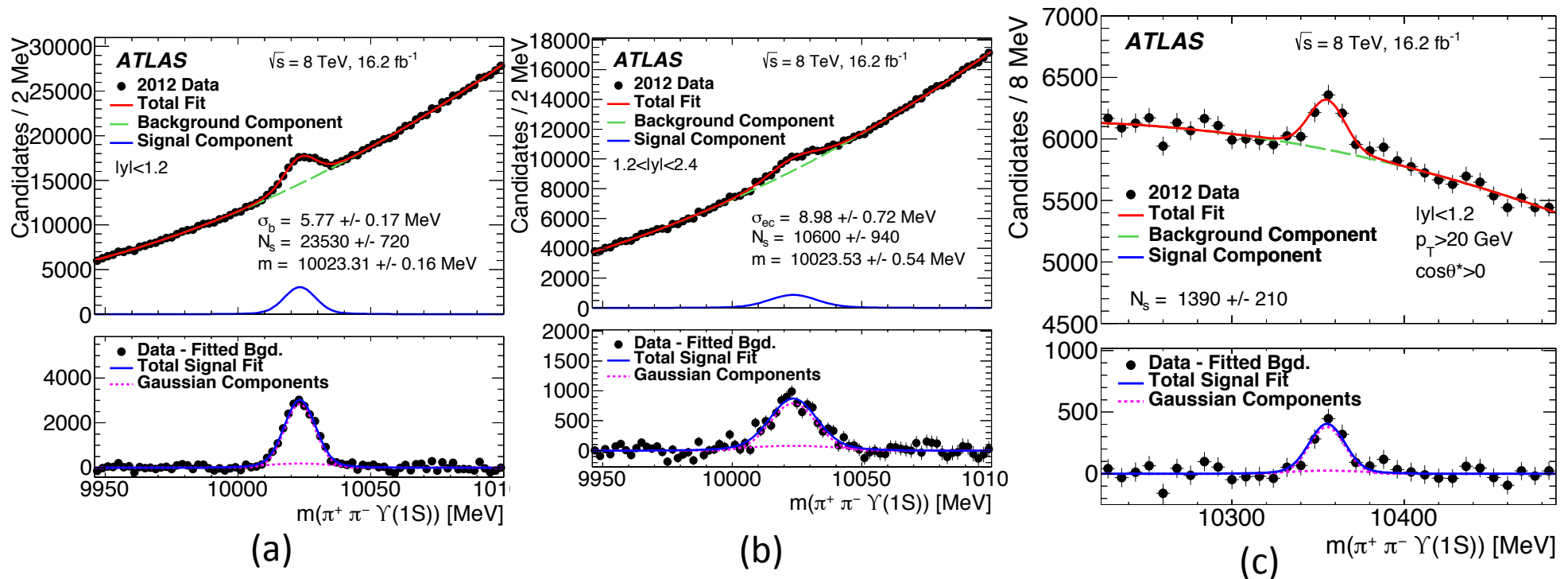
$$R = \frac{[\sigma(pp \rightarrow X_b) B(X_b \rightarrow \pi^+\pi^-\Upsilon(1S))]}{[\sigma(pp \rightarrow \Upsilon(2S)) B(\Upsilon(2S) \rightarrow \pi^+\pi^-\Upsilon(1S))]}$$

Search for the X_b and other hidden-beauty states at ATLAS (1)

- [Physics Letters B 740 \(2015\), pp. 199–217](#)
- 16.2 fb⁻¹ of 8 TeV ATLAS data.
- Search in the decay channel $X_b \rightarrow \pi^+ \pi^- \Upsilon(1S)(\rightarrow \mu^+ \mu^-)$.
- Analysis is performed in eight bins of rapidity, transverse momentum, and the angle (in the rest frame of the parent state) between the dipion system and the laboratory-frame momentum of the parent.

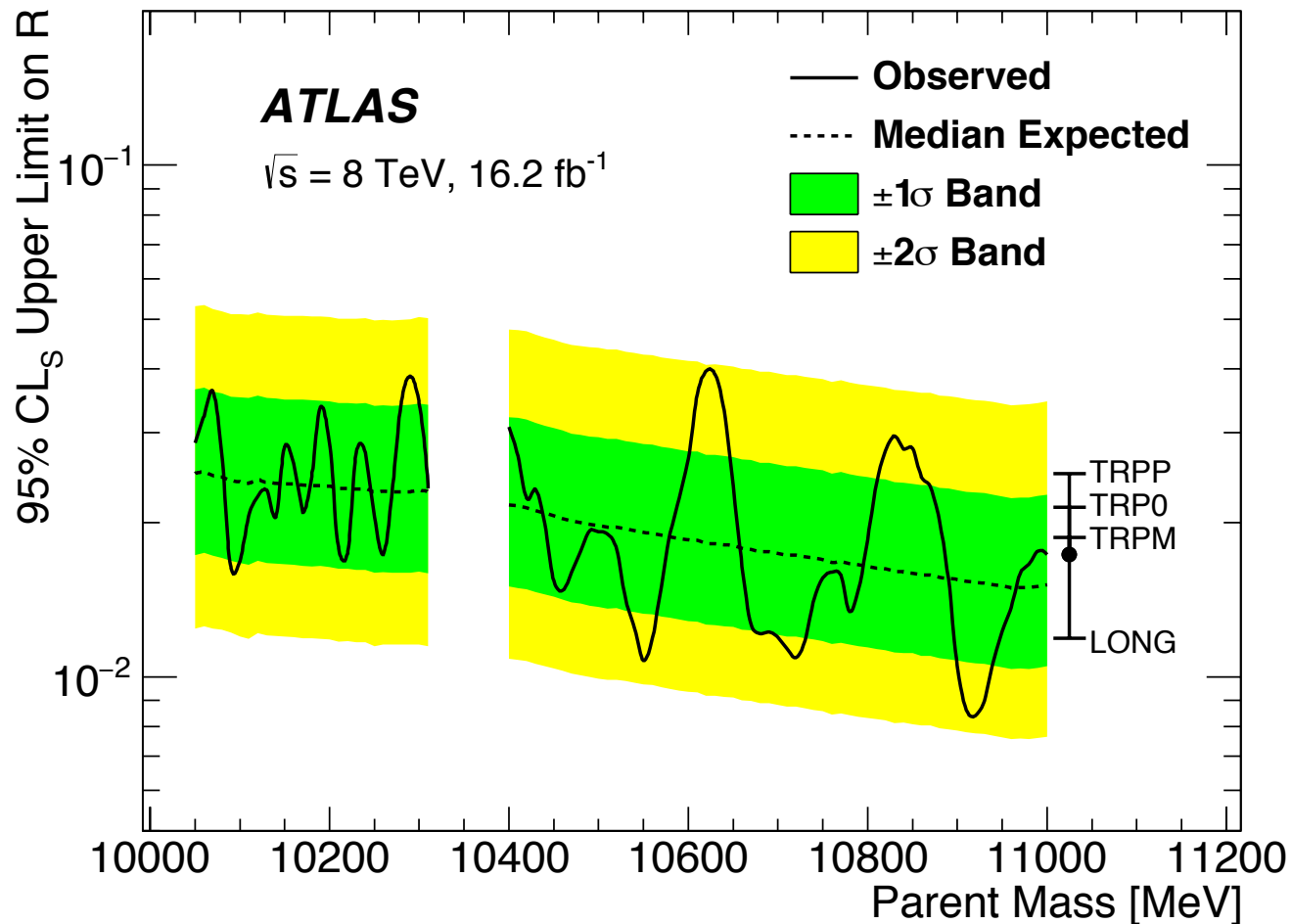


Search for the X_b and other hidden-beauty states at ATLAS (2)



- The signal shape, distribution of signal among analysis bins, and efficiency, are first calibrated on the $\Upsilon(2S)$ peak in data \rightarrow that it turns out only one parameter: the division of signal between barrel and endcap that needs to be adjusted.
- After this, the simultaneous fit to the 8 bins is validated on the $\Upsilon(3S)$.
- Both the expected overall yield and the division among bins are reproduced well.

Search for the X_b and other hidden-beauty states at ATLAS (3)



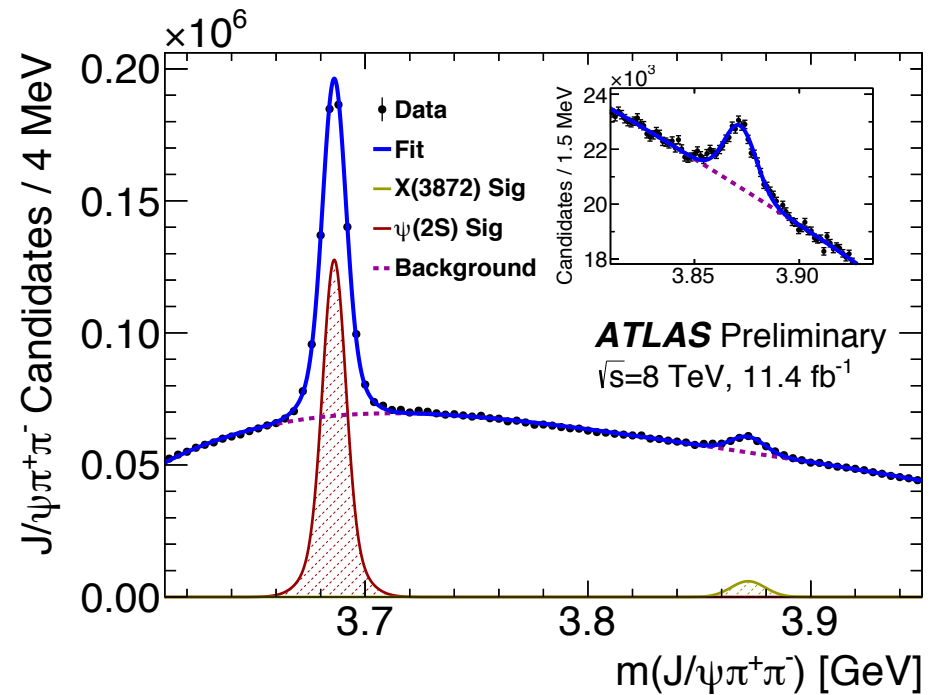
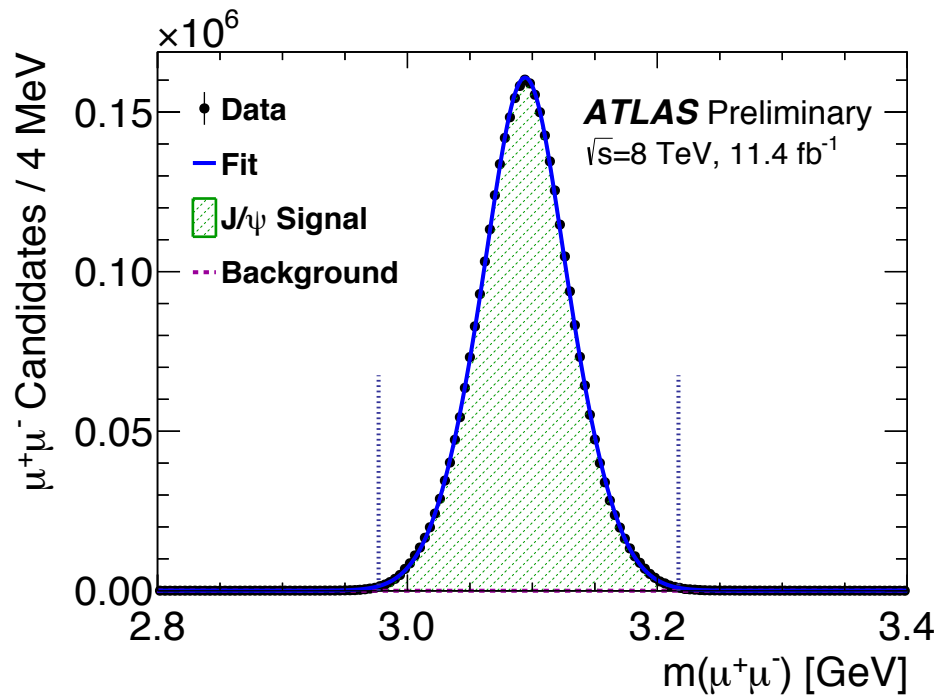
- The bar on the right shows typical shifts under alternative X_b spin-alignment scenarios.
- Upper limits are recalculated under longitudinal ('LONG') and three transverse ('TRPP', 'TRP0', 'TRPM') spin-alignment scenarios.

- No evidence for new narrow states is found for masses 10.05–10.31 GeV and 10.40–11.00 GeV.
- Upper limits are also set on the ratio

$$R = [\sigma(pp \rightarrow X_b) B(X_b \rightarrow \pi^+\pi^-\Upsilon(1S))] / [\sigma(pp \rightarrow \Upsilon(2S)) B(\Upsilon(2S) \rightarrow \pi^+\pi^-\Upsilon(1S))],$$
 with results ranging from 0.8% to 4.0% depending on the X_b mass.

Production measurements of $\psi(2S)$ and $X(3872)$ at ATLAS (1)

- [ATLAS-CONF-2016-028](#)
- Decay mode: $J/\psi \pi^+ \pi^-$, 11.4 fb⁻¹ of 8 TeV ATLAS data.
- Rapidity range $|y| < 0.75$, p_T range of $J/\psi \pi^+ \pi^- = (10 - 70)$ GeV.
- MC simulation is used for studies of selection and reconstruction efficiencies.

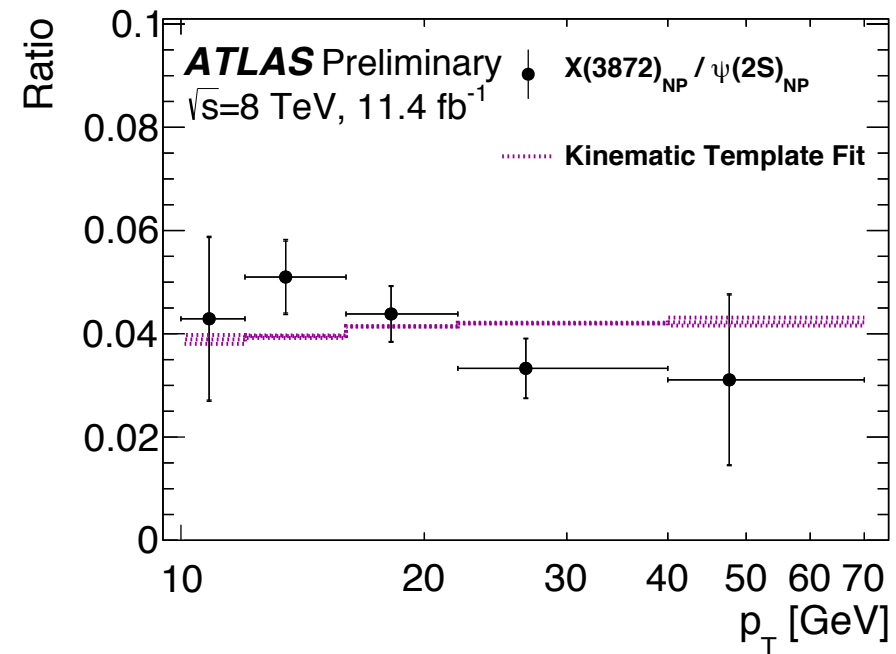
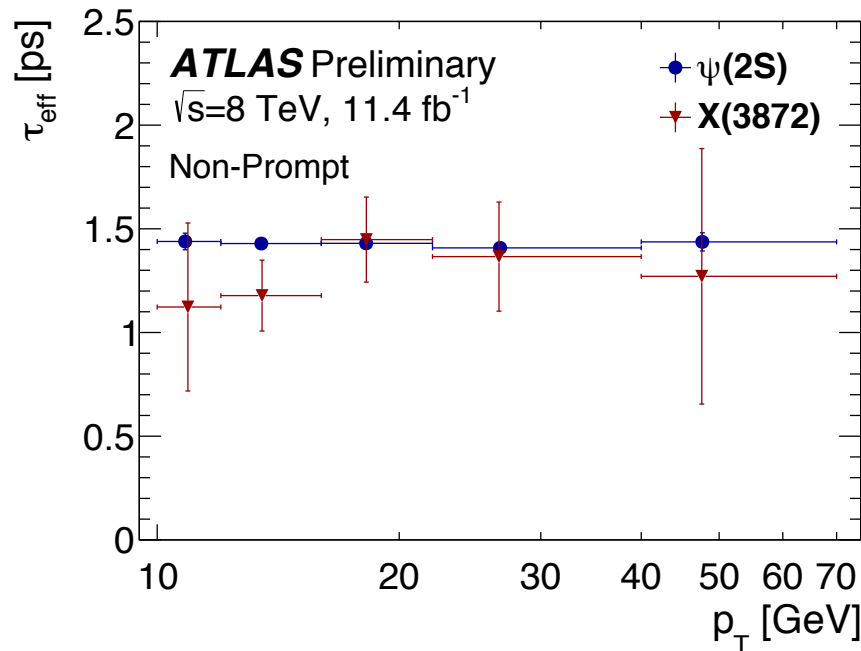


Production measurements of $\psi(2S)$ and $X(3872)$ at ATLAS (2)

- The production cross sections of the $\psi(2S)$ and $X(3872)$ states are measured in five bins of $J/\psi\pi^+\pi^- p_T$, with bin boundaries
 - (10, 12, 16, 22, 40, 70) GeV.
- The cross sections measured are obtained under the assumption of
 - no spin alignment, but
 - appropriate sets of correction factors for a number of extreme spin alignment scenarios are calculated and presented in the Appendix of the corresponding Conference Note.
- In order to separate prompt production of the $\psi(2S)$ and $X(3872)$ states and the non-prompt production from the decays of long-lived particles such as b-hadrons, the data sample in each p_T bin was divided into intervals of pseudo-proper lifetime $\tau=L_{xy}m/p_T$.
- Four intervals of $\tau(J/\psi\pi^+\pi^-)$ were defined:
 - $-0.3 \text{ ps} < \tau < 0.025 \text{ ps}$
 - $0.025 \text{ ps} < \tau < 0.3 \text{ ps}$
 - $0.3 \text{ ps} < \tau < 1.5 \text{ ps}$
 - $1.5 \text{ ps} < \tau < 15.0 \text{ ps}$

Production measurements of $\psi(2S)$ and $X(3872)$ at ATLAS (3)

- Measured effective pseudo-proper lifetimes for non-prompt $X(3872)$ and $\psi(2S)$, and the ratio of non-prompt $X(3872)$ and $\psi(2S)$ production.



- Kinematic template fit was calculated as a ratio of the simulated p_T distributions of non-prompt $X(3872)$ and non-prompt $\psi(2S)$, assuming that the same mix of the parent b-hadrons contributes for both signals.
- The shape of the template reflects the kinematics of the decay of a b-hadron into $\psi(2S)$ or $X(3872)$, with the width of the band showing the range of variation for extreme values of the invariant mass of the recoiling hadronic system.

Production measurements of $\psi(2S)$ and $X(3872)$ at ATLAS (4)

- The fit of the measured ratio to that template allows to determine the ratio of the average branching fractions:

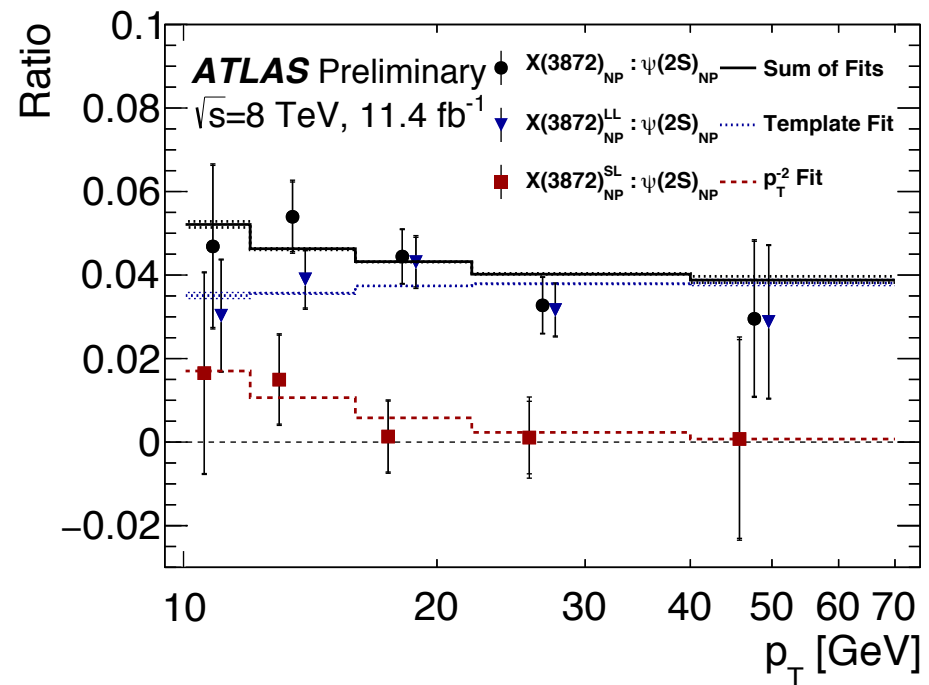
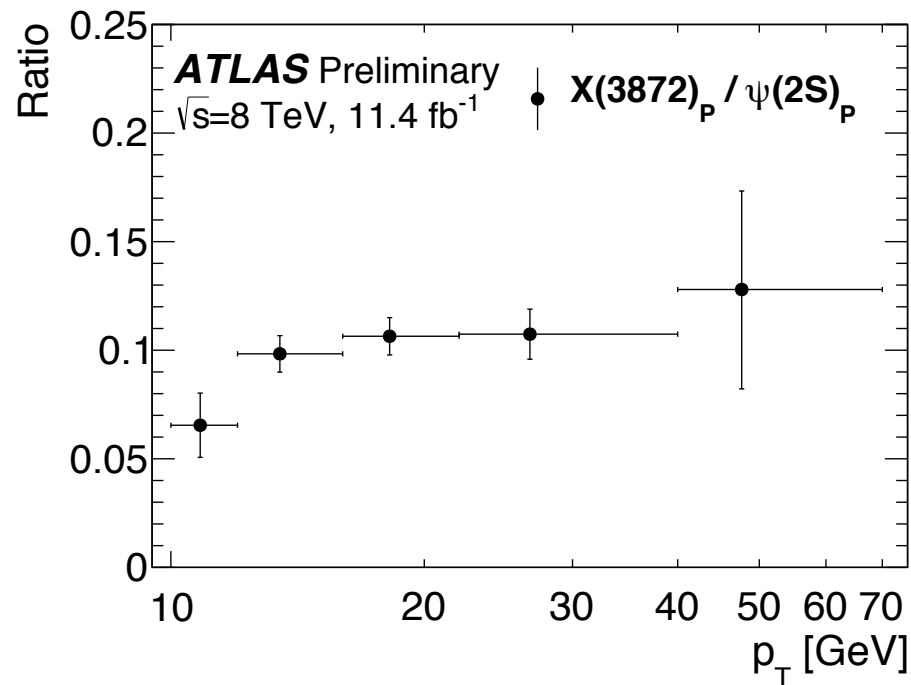
$$R_B^{1L} = \frac{Br(B \rightarrow X(3872))Br(X(3872) \rightarrow J/\psi\pi^+\pi^-)}{Br(B \rightarrow \psi(2S))Br(\psi(2S) \rightarrow J/\psi\pi^+\pi^-)} = (3.95 \pm 0.32(\text{stat}) \pm 0.08(\text{sys}))\%$$

- The somewhat falling trend shown on the right figure on the previous slide does not completely agree with the shape of the template, also **possibly suggesting the presence of an additional contribution** to the non-prompt $X(3872)$ yield in the low- p_T bins.
- The short-lived component is understood to be due to B_c decays, and the value of the pseudo-proper-lifetime parameter of the short-lived component is based on the value expected for B_c .
- An alternative fit model hence was implemented in the analysis, which allows for **two non-prompt contributions** with distinctly different effective lifetimes.

$$R_B^{2L} = \frac{Br(B \rightarrow X(3872))Br(X(3872) \rightarrow J/\psi\pi^+\pi^-)}{Br(B \rightarrow \psi(2S))Br(\psi(2S) \rightarrow J/\psi\pi^+\pi^-)} = (3.57 \pm 0.33(\text{stat}) \pm 0.11(\text{sys}))\%$$

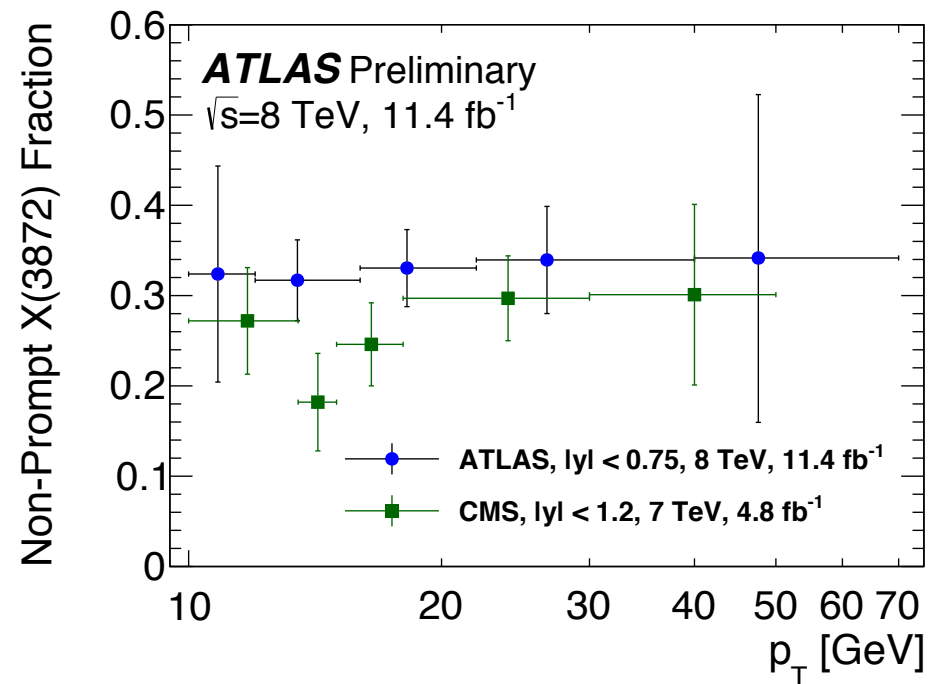
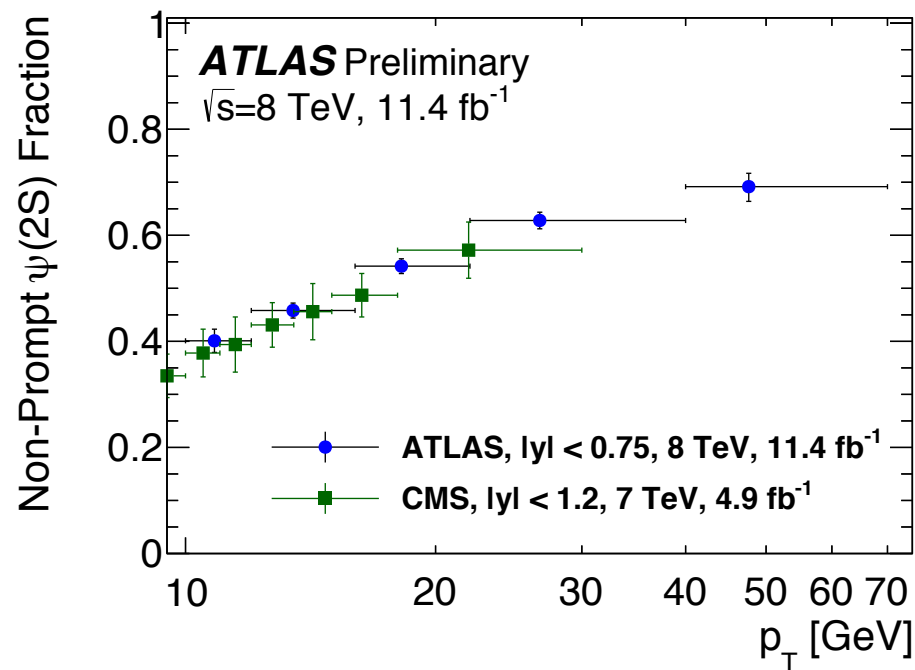
Production measurements of $\psi(2S)$ and $X(3872)$ at ATLAS (5)

- Ratio of cross section times branching fraction between $X(3872)$ and $\psi(2S)$ for prompt (left) and non-prompt (right) production. For the non-prompt production, the total ratio is separated into short-lived and long-lived components for the $X(3872)$.



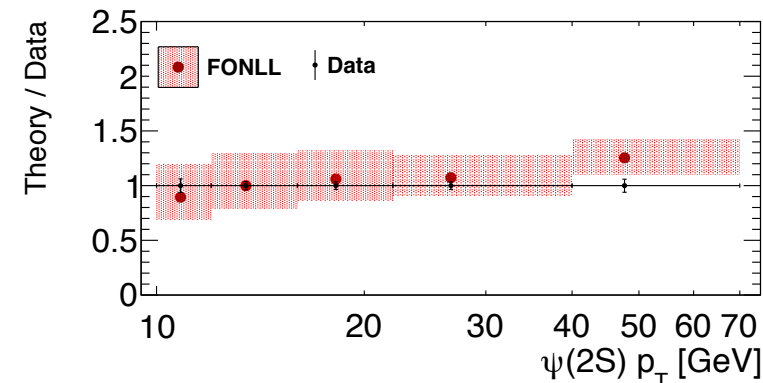
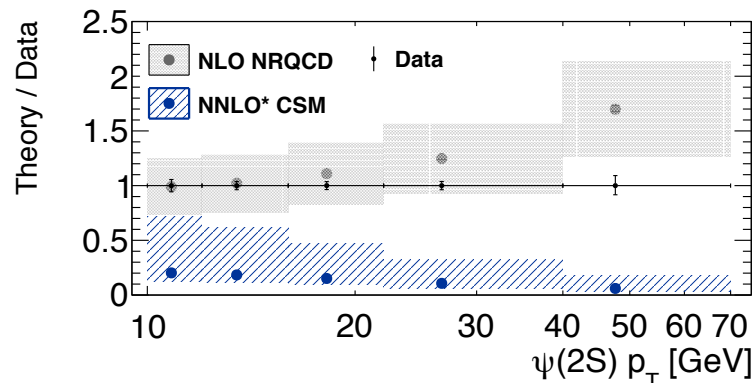
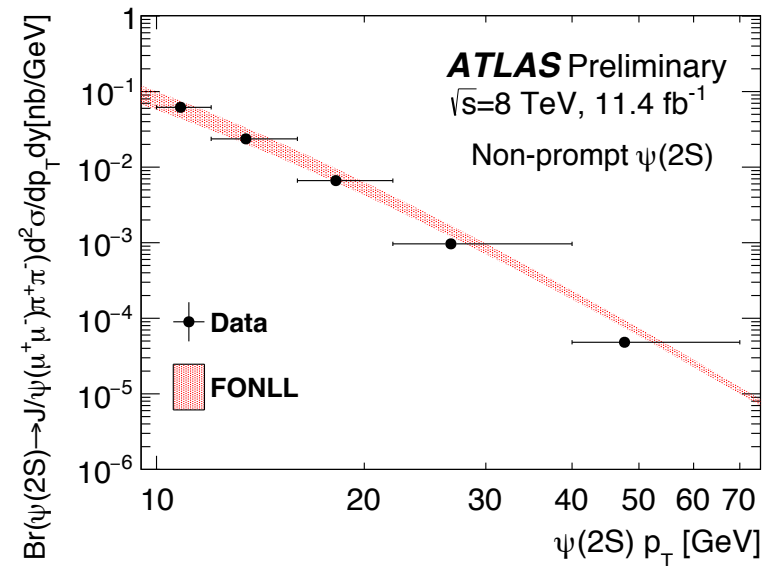
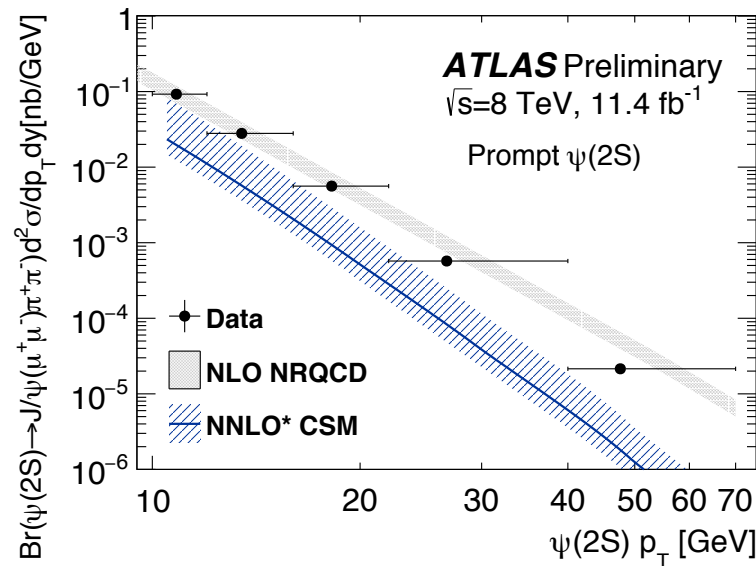
Production measurements of $\psi(2S)$ and $X(3872)$ at ATLAS (6)

- Measured non-prompt fractions for $\psi(2S)$ (left) and $X(3872)$ (right) production, compared to CMS results at $\sqrt{s} = 7$ TeV.



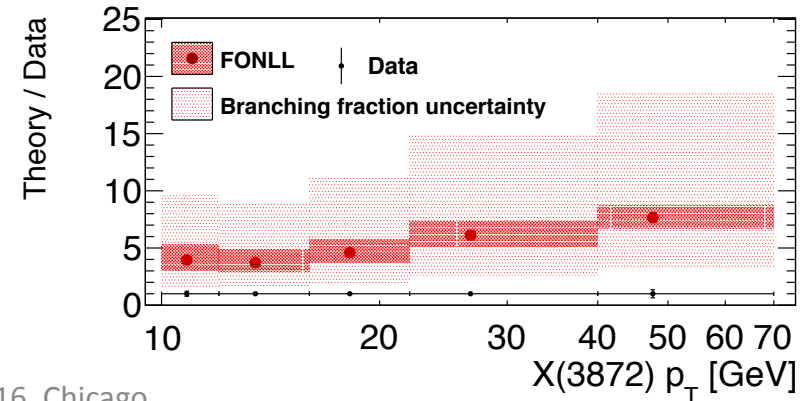
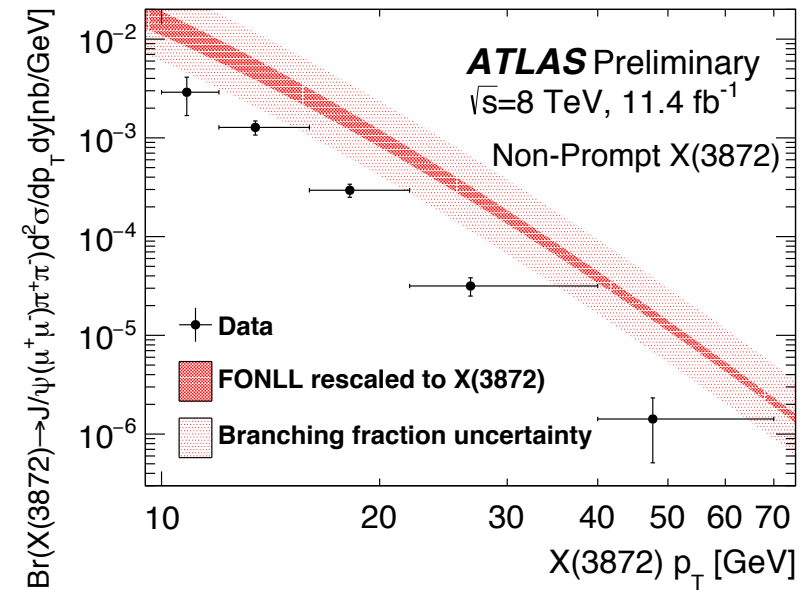
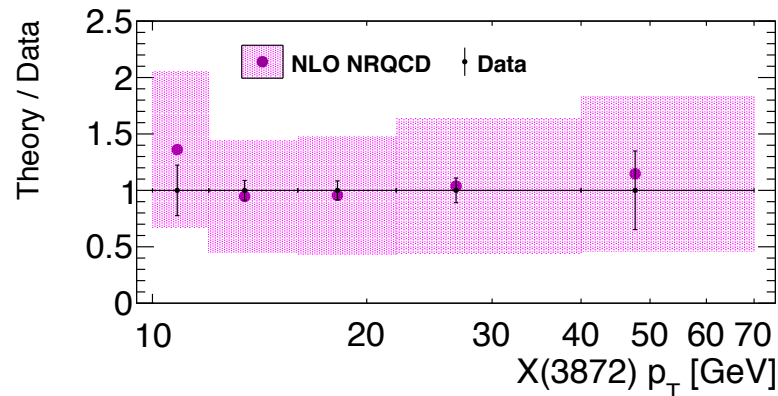
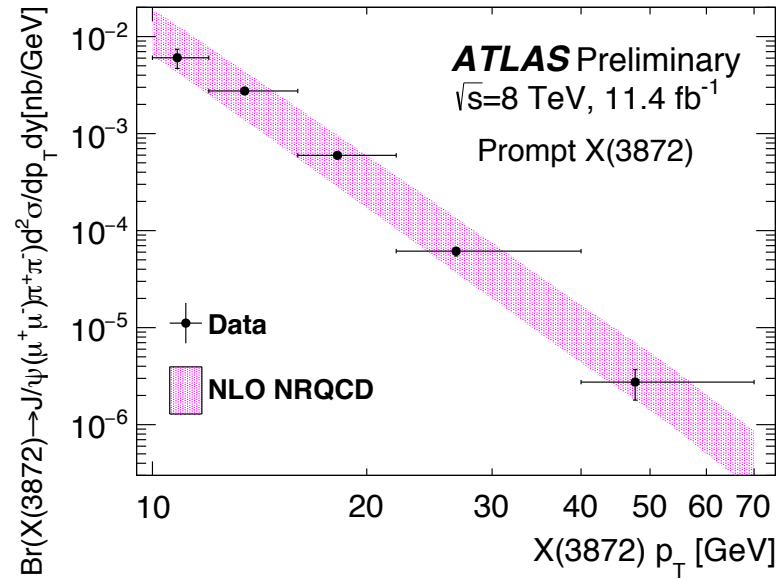
Production measurements of $\psi(2S)$ and $X(3872)$ at ATLAS (7)

- The measured differential cross section (times the product of the relevant branching fractions) for prompt production of $\psi(2S)$ is presented on the left, and the non-prompt production is presented on the right. Compared to NLO NRQCD, NNLO* CSM and FONLL.



Production measurements of $\psi(2S)$ and $X(3872)$ at ATLAS (8)

- The measured differential cross section (times the product of the relevant branching fractions) for prompt production of $X(3872)$ is presented on the left, and the non-prompt production is presented on the right. The $X(3872)$ is modeled as a mixture of a $\chi_{c1}(2P)$ and a $\bar{D}^0 D^{*0}$ molecular state.



Production measurements of $\psi(2S)$ and $X(3872)$ at ATLAS (9)

- The above is used to determine the fraction of non-prompt $X(3872)$ from short-lived sources, integrated over the p_T range ($p_T > 10$ GeV) covered in the analysis:

$$\frac{\sigma(pp \rightarrow B_c) Br(B_c \rightarrow X(3872))}{\sigma(pp \rightarrow \text{non-prompt } X(3872))} = (25 \pm 13(\text{stat}) \pm 2(\text{sys}) \pm 5(\text{spin}))\%$$

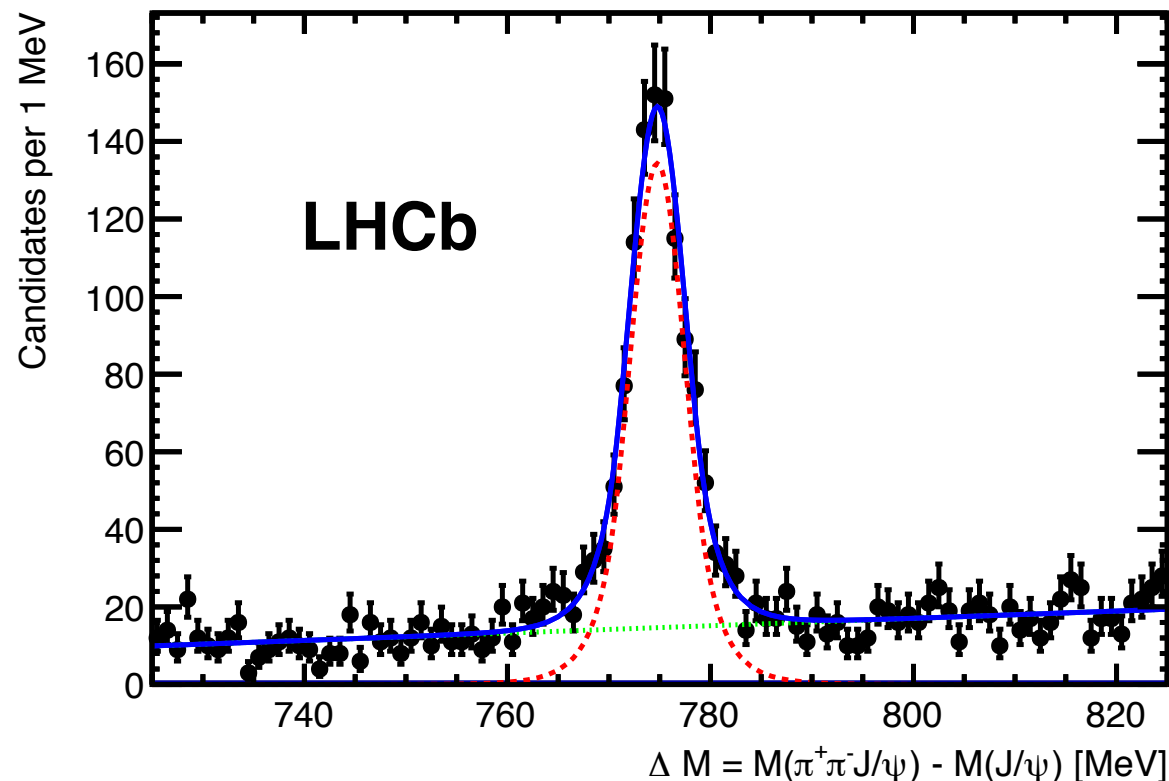
- The invariant mass distributions of the di-pion system in $\psi(2S) \rightarrow J/\psi \pi^+ \pi^-$ and $X(3872) \rightarrow J/\psi \pi^+ \pi^-$ decays are also measured. The results do not favour a phase space distribution in either decay, and favour $X(3872) \rightarrow J/\psi \rho^0$.

X(3872) quantum numbers determination at LHCb (1)

- [Phys. Rev. D 92, 011102 \(2015\)](#)
- Brief history and foreword
 - Early constraints on the quantum numbers – CDF's 2005 angular analysis restricted the options to 1^{++} and 2^{-+} ; also using the dipion mass distribution.
 - [Measurement of the Dipion Mass Spectrum in X\(3872\) \$\rightarrow\$ J/ \$\psi\$ \$\pi\pi\$.](#)
 - In 2011 these numbers are confirmed by Belle.
 - LHCb's 2013 full angular analysis finally settled on 1^{++} , but that analysis assumed that the lowest orbital angular momentum process dominated the decay.
 - [Phys. Rev. Lett. 110 \(2013\) 222001.](#)
 - The new analysis presented below removes that assumption.

X(3872) quantum numbers determination at LHCb (2)

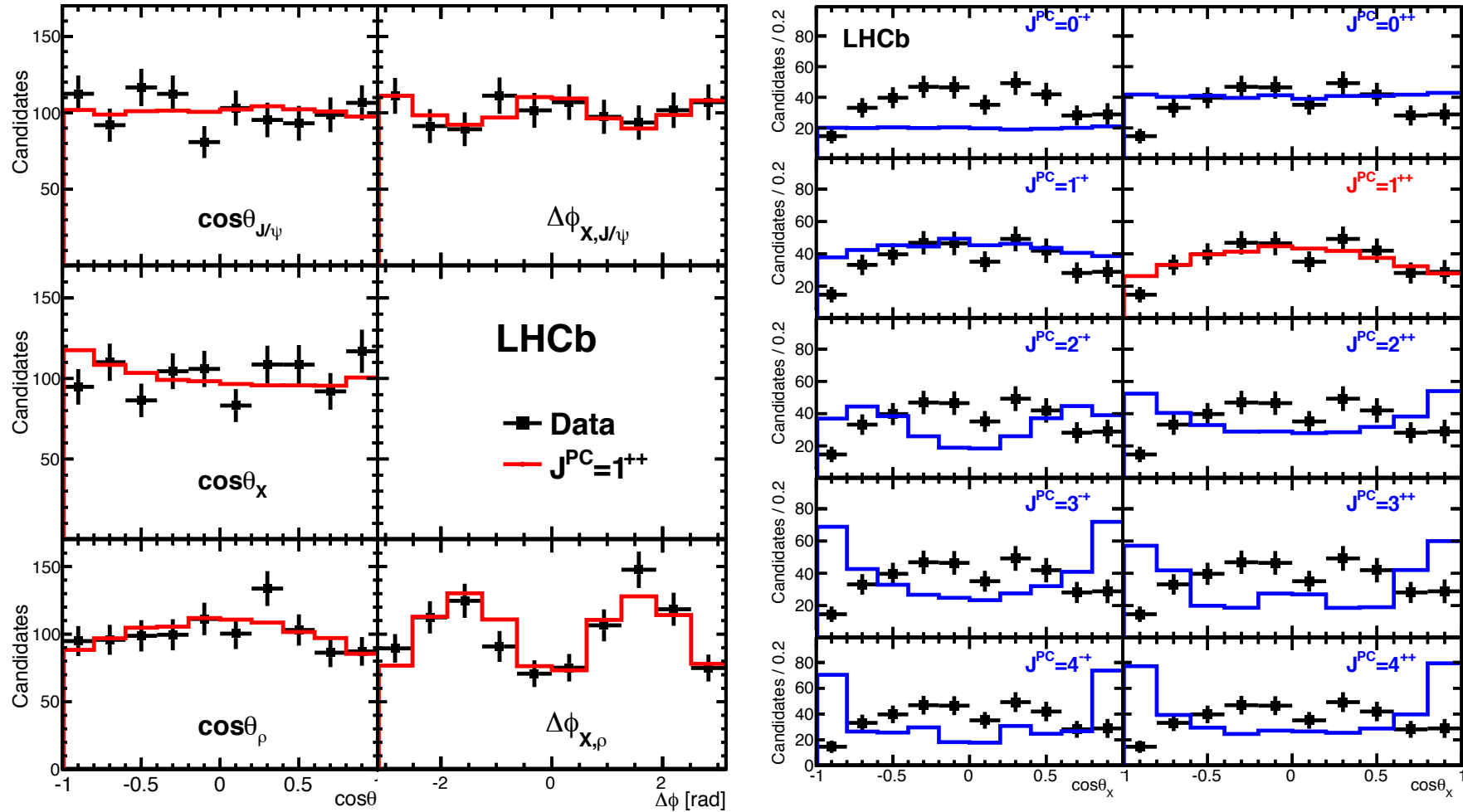
- 3.0 fb⁻¹ of 7 and 8 TeV LHCb data.
- $B^+ \rightarrow X(3872)K^+$, with $X(3872) \rightarrow \rho^0 J/\psi$, $\rho^0 \rightarrow \pi^+\pi^-$ and $J/\psi \rightarrow \mu^+\mu^-$.
- The fit yields 1011 ± 38 signal events over the background of 1468 ± 44 in the ΔM range of (725–825) MeV. The X(3872) mass resolution is 2.8 MeV.
- The signal purity is 80% within 2.5σ around the peak.



X(3872) quantum numbers determination at LHCb (3)

- The probability density function P for each J^{PC} hypothesis, J_X , is defined in the five-dimensional angular space
 - $\Omega \equiv (\cos\theta_X, \cos\theta_\rho, \Delta\phi_{X,\rho}, \cos\theta_{J/\psi}, \Delta\phi_{X,J/\psi})$, where
 - θ_X , θ_ρ and $\theta_{J/\psi}$ are the helicity angles in X(3872), ρ_0 and J/ψ decays, respectively, and
 - $\Delta\phi_{X,\rho}$, $\Delta\phi_{X,J/\psi}$ are the angles between the decay planes of the X(3872) particle and of its decay products.
- The quantity P is the normalized product of the expected decay matrix element M squared and of the reconstruction efficiency (ε), $P(\Omega|J_X) = |M(\Omega|J_X)|^2 \varepsilon(\Omega)/I(J_X)$, where $I(J_X) = \int |M(\Omega|J_X)|^2 \varepsilon(\Omega) d\Omega$.
- In this analysis both S- and D-wave contributions are allowed.
- The background is subtracted using the sPlot technique.
- The 1^{++} hypothesis gives the highest likelihood value, as shown on the next slide.

X(3872) quantum numbers determination at LHCb (4)



- Left: background-subtracted distributions of all angles for the data (points with error bars) and for the 1^{++} fit projections (solid histograms).
- Right: Background-subtracted distribution of $\cos\theta_X$ for candidates with $|\cos\theta_\rho| > 0.6$ for the data (points with error bars) compared to the expected distributions for various $X(3872)$ J^{PC} assignments (solid histograms).

X(3872) quantum numbers determination at LHCb (5)

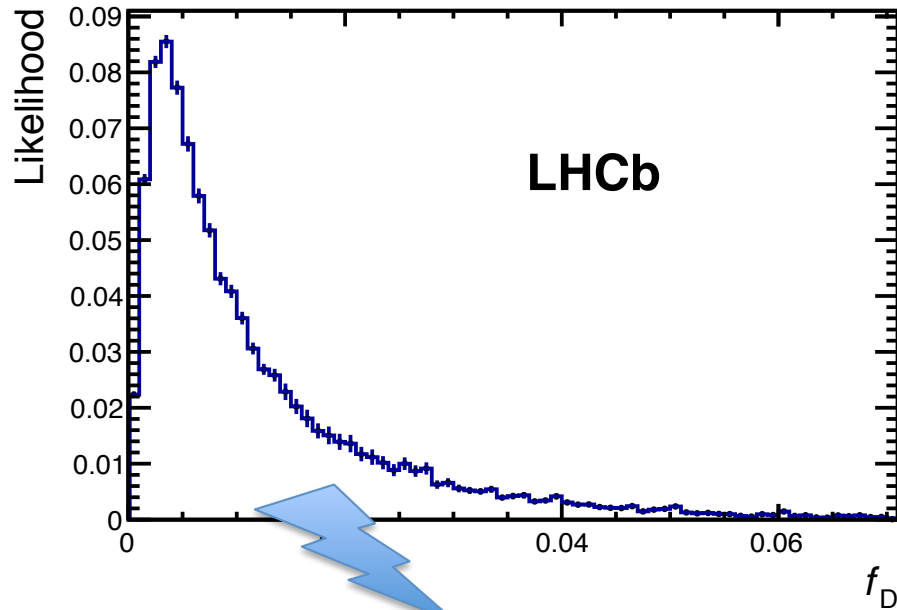
- The analysis confirms that the eigenvalues of total angular momentum, parity and charge-conjugation of the $X(3872)$ state are 1^{++} .
- These quantum numbers are consistent with those predicted by the molecular or tetraquark models and with the $\chi_{c1}(2^3P_1)$ charmonium state, possibly mixed with a molecule. Other charmonium states are excluded.
- No significant D-wave fraction is found, with an upper limit of 4% at 95% C.L.
- The S-wave dominance is expected in the charmonium or tetraquark models, in which the $X(3872)$ state has a compact size. An extended size, as that predicted by the molecular model, implies more favorable conditions for the D-wave.

Conclusions

- LHC experiments have a rich program for studies of the $X(3872)$ and other exotic hadron states.
- ATLAS has recently provided a comprehensive study of $X(3872)$ and $\psi(2S)$ production.
- LHCb has determined the quantum numbers of the $X(3872)$ and separated the S- and D-wave modes; made the first production cross-section measurement in pp collisions, a precise mass measurement, an evidence of $X(3872) \rightarrow \psi(2S)\gamma$ and a search for $X(3872) \rightarrow p\bar{p}$.
- CMS and ATLAS have performed searches for the X_b , the $X(3872)$ bottomonium counterpart.

BACKUP

X(3872) quantum numbers determination at LHCb (6)



Likelihood-weighted distribution of the D-wave fraction. The distribution is normalized to unity.

Background-subtracted distribution of $\cos \theta_X$ for candidates with $|\cos \theta_\rho| > 0.6$ for the data (points with error bars) compared to the expected distributions for various $X(3872) J^{PC}$ assignments (solid histograms) with the B_{LS} amplitudes obtained by the fit to the data in the five-dimensional angular space. The fit displays are normalized to the observed number of the signal events in the full angular phase space.

